Advances in Science and Technology Research Journal

Advances in Science and Technology Research Journal, 2026, 20(3), 213–225
https://doi.org/10.12913/22998624/214033
ISSN 2299-8624, License CC-BY 4.0

Received: 2025.09.03
Accepted: 2025.11.06
Published: 2026.02.01

Investigation of shock wave effect on activation of a pressure-sensitive landmine fuze

Vitalii Myntiuk[1], Olga Shypul[1*], Oleksiy Pavlenko[1], Denys Tkachenko[1], Vadym Garin[1], Dmytro Brega[1]

[1] Faculty of Aircraft Building, National Aerospace University Kharkiv Aviation Institute, Vadyma Manka Str. 17, 61070, Kharkiv, Ukraine
* Corresponding author's e-mail: o.shipul@khai.edu

ABSTRACT

The study investigated how shock wave parameters, specifically impulse and pressure amplitude, affect the fuze of a landmine. This research is driven by the need to develop an effective method for contactless gas detonation demining. In this method, detonating a gas mixture within demining device tubes produces shock waves with sufficient intensity to trigger a mine. Most fuzes, specifically pressure-acting, are produced from thermosetting plastics like Bakelite and are designed to activate under quasi-static loading. Therefore, it is essential to evaluate its behaviour when exposed to short-term pressure impulses generated by the shock waves from a contactless demining device. The investigation employed numerical modelling and experimental verification. A three-dimensional finite element model of the landmine fuze was developed using experimentally validated material properties and a Friedlander-type loading form. The simulations were conducted in the LS-DYNA environment. The results showed that the destructive effect of the shock wave is mainly driven by the pressure impulse, which needs to be above 40 Pa·s for activation to happen. Although pressure amplitude has a lesser effect, increasing it can improve the activation of a fuze. The ability of the developed contactless demining device to trigger the fuze of the tested mine type has been confirmed through experiments. While the pressure amplitude has a lesser impact than the pressure impulse, it has been established that increasing it also activates the fuze. The ability of the newly developed contactless demining device to activate the fuse of the mine of the type under study was experimentally proven.

Keywords: blast load, contactless gas detonation demining device, demining, detonation wave, FEM simulation, fuze, landmine, mine defusing.

INTRODUCTION

The current reality is increasingly directing applied science towards developing methods to enhance the defence capabilities of countries, including engineering solutions for humanitarian demining in contaminated areas. There are currently two methods of demining: manual and mechanisation. Manual demining is conducted by sappers, which is both slow and dangerous. Given the critical importance of highly qualified specialists, manual methods are primarily employed in difficult terrains that are inaccessible to mechanised equipment. The mechanised approach to mine clearance involves the use of specialised machines and can be broadly categorised into contact and contactless methods. Numerous contact-action demining machines exist [1], but they share a common drawback: the short lifespan of their working parts (such as rolls and chains). Alternative approaches to mine neutralisation have also been investigated. Zaichenko et al. [2] highlighted the demand for safer and more cost-effective solutions, proposing a hydrodynamic device that neutralises mines by means of an electric discharge in a liquid medium. Pratt and Torbet [3] explored the use of a hybrid thermal lance for in situ deflagration of mines, while Vega et al. [4] experimentally confirmed the effectiveness of high-power electromagnetic radiation for neutralising

improvised explosive devices (IEDs). Wang et al. [5] reviewed both passive and active explosion suppression methods in confined environments, offering the insights that can be adapted to improve mine safety systems. UAV-based techniques are likewise gaining traction: Tabassum et al. [6] demonstrated that drones equipped with advanced imaging technologies can significantly accelerate and enhance the safety of post-conflict landmine clearance.

Among the known contactless demining methods, one of the most promising involves using directed gas detonation to impact mine fuze remotely. This method works by initiating the detonation of a gas mixture in tubes, generating a shock wave that activates the mine fuze, resulting in its neutralization. The primary advantage of this technique is that it allows for the contactless activation of mine detonation without requiring direct contact with the mine itself, significantly reducing the destructive impact on the structure of a demining device caused by the shock wave produced by the mine explosion [7]. In [8], the authors of this study presented a conceptual model of an efficient, safe, autonomous and economical contactless gas detonation demining device capable of long-term operation without refuelling or additional maintenance.

The directed gas detonation method is used for demining subjects the fuze to a brief dynamic load in the form of a shock wave. This shock wave is characterised by a short front, high amplitude (reaching up to tens of megapascals), and lasts for milliseconds. When developing this type of demining device, it is important to consider that mine fuzes are typically designed to be activated by quasi-static pressure, particularly when tracked or wheeled vehicles run over them. According to the paper [9], anti-tank landmines (or Improvised Explosive Devices, IEDs) usually utilise pressure-acting fuzes that detonate when a force of approximately 1200–3000 N is applied to the pressure plate. This raises an important question: can such a shock wave generate sufficient mechanical impact to trigger the fuse? To answer this, it is necessary to investigate the interaction between the gas detonation wave and the fuse structure, considering the wave pressure, impulse duration, and the mechanical characteristics of the fuze material.

Thermosetting plastics, such as phenol formaldehyde resin (Bakelite), are widely used in the manufacturing of landmine fuse bodies [10]. This choice reduces the number of metal components, making them harder to detect with metal detectors. Most studies on the impact of explosive loads on plastic products are primarily experimental and focus on countering explosions. For instance, study [11] examined the optimisation of explosion-resistant sandwich panels through numerical experiments. Another investigation [12] explored how using composite reinforcement can enhance explosion resistance.

Research has also been conducted on the effects of explosions on rectangular plates, including composite materials. In this context, the authors highlight the challenge of scaling results to apply them to real structures [13]. Furthermore, experimental studies of composites reveal that the type of fibre used significantly influences key fracture mechanisms and their progression in fiberglass plastics subjected to explosive loading. Interestingly, despite the rapid loading conditions, the mechanical characteristics of these materials remain consistent with the results from quasi-static tests [14]. Additionally, it is noted [15] that even minor inhomogeneities in polymer composites can generate high-stress concentrations that lead to local fractures.

A more comprehensive review of the research on the explosion resistance of heterogeneous systems, including particulate composites, can be found in [16].

It is important to note that most of the studies focus on the effects of shock waves on samples in the shape of rectangular or circular plates. This means they do not address the complex three-dimensional configurations that are characteristic of the mine fuzes examined in this study. The current investigation bridges the gap of understanding how a Bakelite fuse complex case responds to a short-term pressure impulse from gas detonation waves.

RESEARCH METHODOLOGY

This paper investigated the ability to activate mine fuse using a shock wave generated by a contactless gas detonation demining device. Both numerical simulations and field experiments were conducted for this purpose.

Numerical modelling of the transient shock wave impact on mine fuse design was carried out with LS-DYNA version R14.1 (build 115362, build date: 2024-05-29) [17]. A dynamic solver,

which performs explicit integration of the equations of motion, ensuring convergence of solutions for fast-moving and highly nonlinear problems, was used. The creation of a finite element model involves several steps: mesh construction, specifying the mechanical properties of materials, applying loads, and constraining the model.

Full-scale tests to assess the potential for destroying the mine fuze using this method were conducted on an experimental setup equipped with a detonation tube of a demining device. The experimental test plan included tasks such as measuring the pressure of the shock wave along the detonation tube, measuring the pressure of the shock wave on the surface of the mine fuze, and testing for the destruction of the mine fuze.

Numerical simulations description

Finite element mesh

The finite element mesh of an MVP-62 landmine fuze (Figure 1a) is created by breaking down its three-dimensional geometric model into finite elements. The model under study includes the pressure plate, housing, striker and striker spring itself (Figure 1b). This configuration is adequate for modelling the firing mechanism of landmine detonation, which can occur under the following scenarios:

- the pressure plate breaks;
- the plate presses down on the top of the striker;
- the "ears" of the striker, which rest on the case, break off;
- activated by the firing spring, the firing pin impacts the fuse capsule, thereby initiating the subsequent detonation sequence of the mine.

A cross-section of the geometric model is shown in Figure 1c. The calculated finite element mesh is shown in Figure 2a. The mesh consists of tetragonal ten-node elements with five integration points (type 16, [18]). These elements provide enhanced accuracy in approximating solutions, are free from the hourglass effect, and ensure stable convergence without excessive mesh refinement, as well as they reproduce curved surfaces and complex geometries with greater precision and facilitate the generation of high-quality meshes for bodies of arbitrary shape. The average size of the finite elements in the volume of the case and the lower part of the pressure plate is 0.8 mm, and in the rest of the parts that are potentially subject to destruction, it is 0.3 mm. The choice of these finite element sizes is based on the study of the convergence of the support reaction when pressure is applied to the upper surface of the pressure plate. The reaction was chosen as a criterion for assessing accuracy, because it represents the equivalent of the force required to trigger the detonator. The maximum value of the support reaction during a uniform increase in pressure is determined by the time when the fuze pressure plate is destroyed. The dependence of the maximum value of the reaction on the size of the finite element in the thin walls of the fuse pressure plate is shown in Figure 2b. As can be seen, reducing the size of the element from 0.7 mm to 0.1 mm does not significantly refine the reaction value. The magnitude of the reaction changes by 4.5%, from 3287 N for the element size of 0.7 mm to 3145 N for the element size of 0.1 mm. Thus, it is believed that the above-mentioned finite element mesh sizes are sufficient to ensure the required accuracy of the numerical solution.

Material properties

Bakelite is a composite material made from phenol-formaldehyde resin combined with various fillers, such as wood flour, fabric, or mineral fibres. This composition results in a wide range of mechanical properties. However, materials of this

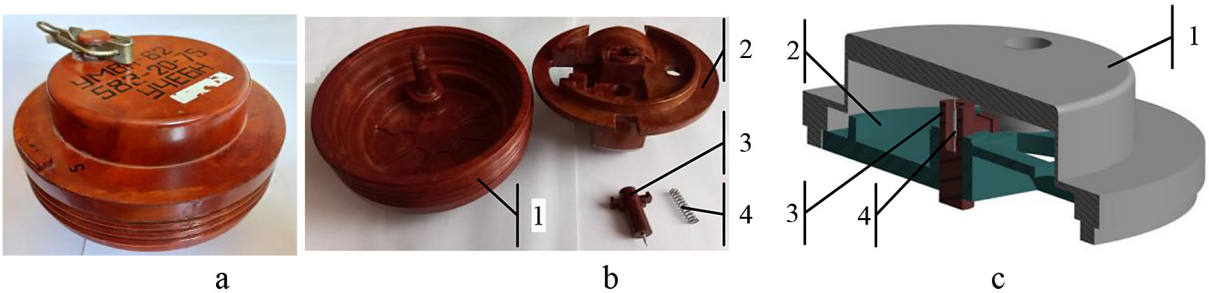

Figure 1. Mine fuse of the MVP-62 landmine: (a) general view; (b) parts included in the model under study; (c) 3D model in section (1 – pressure plate; 2 –housing; 3 – striker; 4 – striker spring)

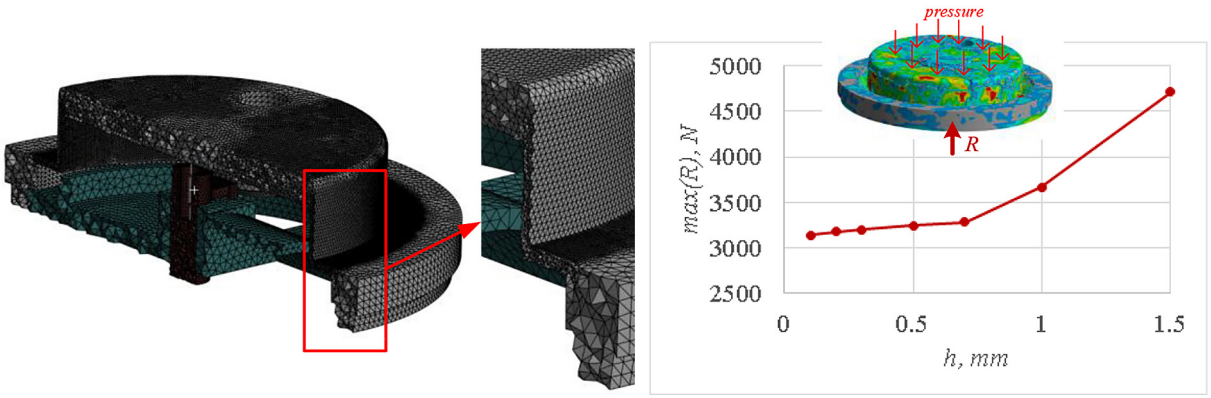

Figure 2. Finite element mesh: (a) general view; (b) convergence of the maximum reaction value from the finite element size

type tend to exhibit brittle fracture without significant plastic deformation, as demonstrated by the notable difference between their tensile and compressive strengths. According to different manufacturers, ordinary Bakelite has the following mechanical properties: compressive strength ranging from 170 MPa to 260 MPa, tensile strength from 50 MPa to 100 MPa, elastic modulus between 8000 MPa and 16000 MPa, and density of 1300 kg/m³ to 1500 kg/m³.

To calibrate these characteristics, one can use the pressing force required to trigger the fuze. Regulatory documents specify the magnitude of this force in the range of 1200 N to 3000 N, which is consistent with the data reported in [9]. The wide variation in this range suggests uncertainty regarding the mechanical properties of Bakelite and/or significant deviations in its nominal dimensions. More precise values, also outlined in regulatory documents, indicate a force of 180 N to 250 N, which is the threshold at which the "ears" of the striker break off. The upper end of this range is more conservative and is used to calibrate the mechanical characteristics of Bakelite.

For this study, the average values of the mechanical characteristics mentioned above were used, except for the tensile strength (see Table 1). This value was selected to ensure that the "ears" of the striker would break off when a force of 250 N is applied. To facilitate modelling, a quarter of the striker and a quarter of the housing part were chosen for symmetry (refer to Figure 3a). A force is applied to the upper surface of the striker, while the lower surface of the housing is fixed. The breaking force of the "ears" is determined by measuring the reaction force at the support (see Figure 3b). Consequently, the mechanical characteristics of the fuze material listed in Table 1 indicate that it will operate under a pressing force of 63.7 N, which translates to approximately 255 N (calculated as 63.7 N

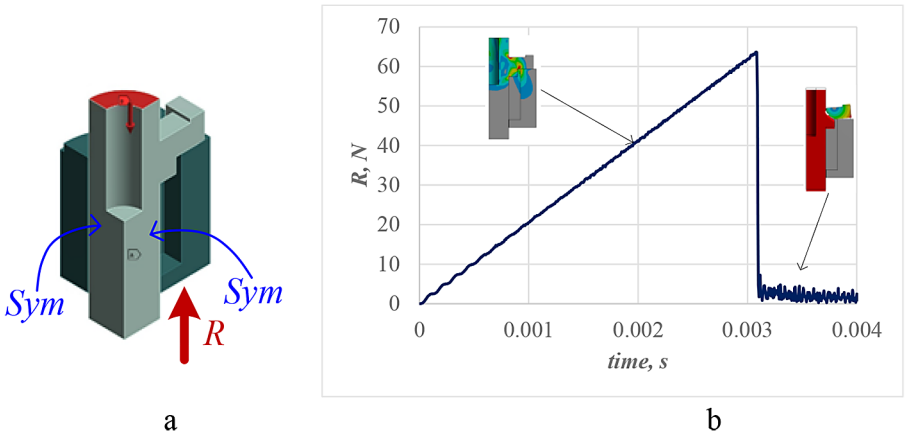

Figure 3. Numerical experiment to determine the breaking force of the striker's "ear": (a) model; (b) reaction growth over time and determination of the maximum value (63.7 N)

Table 1. Material properties

Density, kg/m³	Young's Modulus, MPa	Ultimate strength, MPa	
		Tensile	Compressive
1400	8500	60	225

x 4), closely aligning with the value specified in the regulatory documents. Moreover, the mechanical characteristics accepted (detailed in Table 1) result in a static fracture force of 3150 N, slightly exceeding the upper limit stipulated in the regulations. As there is no plastic deformation anticipated, the material is assumed to behave in a linear elastic manner [19] (*MAT_ELASTIC). The strength limits are defined by the *MAT_ADD_EROSION keyword, which establishes the criteria for the destruction (removal from the model) of finite elements.

Loads and constrains

The nodes on the surfaces shown in Figure 4a are fixed and do not allow any movement. The highlighted surfaces correspond to the locations of the thread that attaches fuze to the mine, as well as the fixation of all parts of the fuse using a locking ring. It is assumed that the pressure is evenly distributed over the surface of the plate (see Figure 4b). The variation in pressure over time follows the standard Friedlander waveform (refer to Figure 4c), which can be expressed using a specific formula:

$$p = P_s\left(1 - \frac{t}{T_s}\right)\mathrm{e}^{-\frac{bt}{T_s}} \tag{1}$$

where: P_s is the peak pressure; T_s is the positive phase duration and b is the decay coefficient.

Excess pressure impulse, known as the positive impulse, is defined as the integral of the excess pressure curve during the positive phase (T_s):

$$I = \int_0^{T_s} p = \frac{TsPs}{b^2}\left(b - 1 + \mathrm{e}^{-b}\right) \tag{2}$$

On the basis of the formulas (1) and (2), there are four parameters for studying the shock wave: P_s, T_s, b, and I. It is important to note that variations in the parameters T_s and b have a nearly identical effect on the shape of the pressure curve. This can be observed in the graphs shown in Figure 5a, which displays pressure profiles with different durations for the positive phase (T_s) and different decay coefficients (b), while keeping the amplitude (P_s) and impulse magnitude (I) constant. Similar conclusions can be drawn by comparing the graphs shown in Figure 5b and 5d. In both cases, the amplitude (P_s) is altered, while the impulse value (I) remains unchanged. In the first instance, the change is due to the duration of the positive phase (T_s), while in the second, it is due to the decay coefficient (b). As a result, nearly identical pressure distributions over time were achieved in both scenarios. Thus, the conducted investigation can be simplified into two cases: one with a variable impulse at a constant amplitude (illustrated in Figure 5c) and the other with a variable amplitude at a constant impulse (shown in Figure 5d). The parameter values are chosen to closely approximate the pressure and duration of the positive phase that occur during the detonation of oxygen-acetylene or propane mixtures.

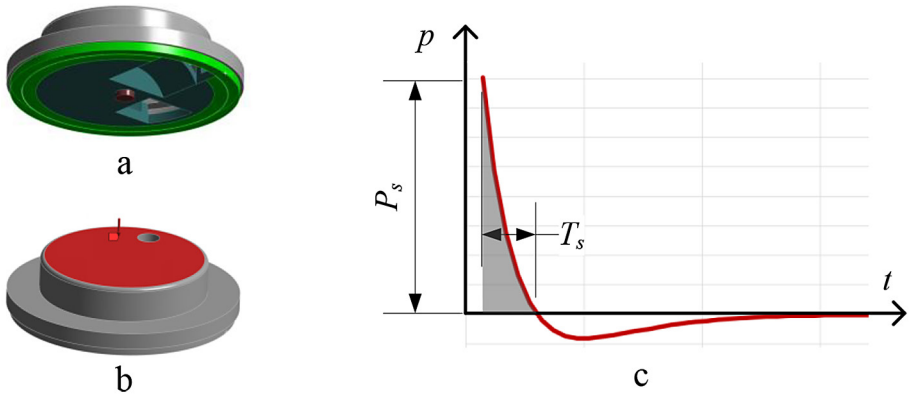

Figure 4. Load and constrained: (a) fixed surfaces; (b) pressure load; (c) pressure change over time

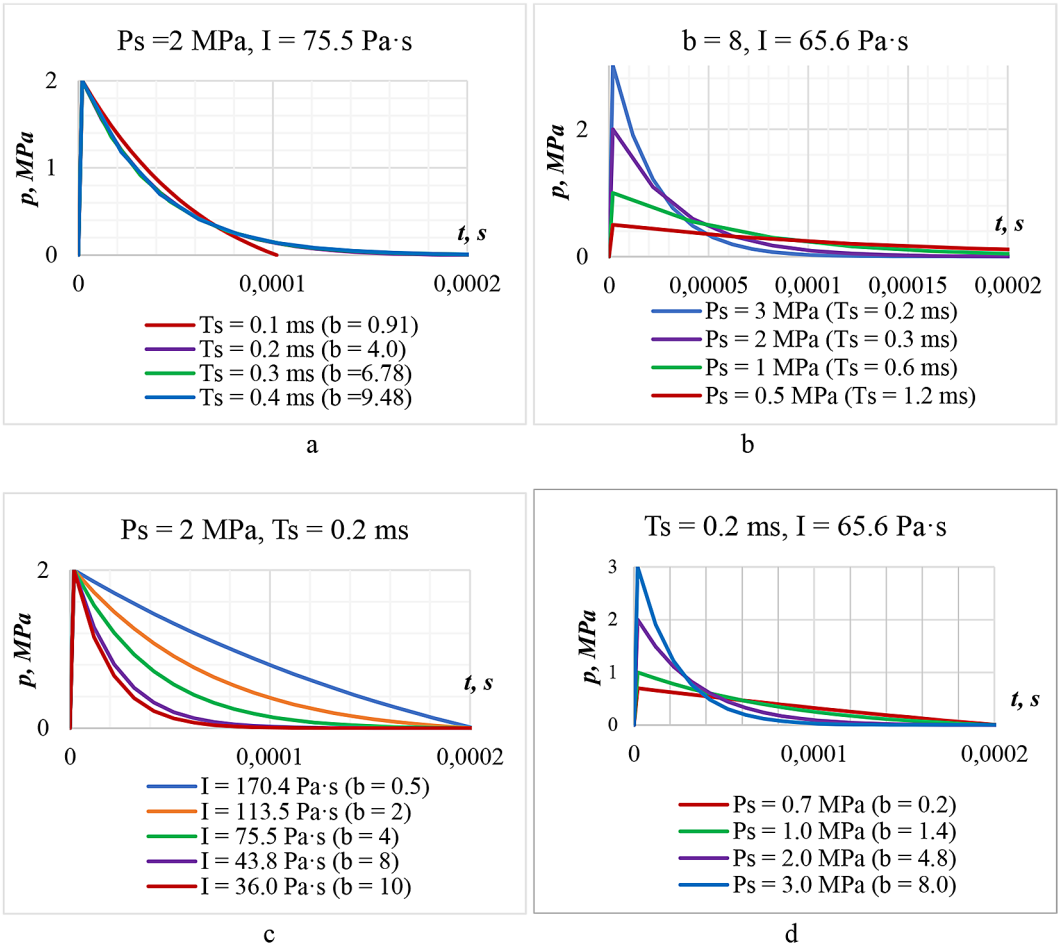

Figure 5. Shock wave shapes for planning a numerical experiment to determine the impact of the blast wave parameters on the fuse under the condition: (a) of constant amplitude and impulse; (b) of constant decay coefficient and impulse; (c) of constant amplitude and duration of the positive phase; (d) of constant impulse and duration of the positive phase

Experimental setup description

The experimental setup consists of a 1 m long detonation tube with an internal diameter of 92 mm, a fuel mixture supply system, an ignition system, and pressure measurement sensors connected to the measuring equipment. The scheme of the experimental setup is presented in Figure 6. The detonation tube was filled with a mixture of acetylene and oxygen (C_2H_2+O_2). The composition of the mixture approached stoichiometric, where the mixture of acetylene to oxygen was 2:5. The combustible mixture has no overpressure, and its temperature was the same as the ambient temperature of 25°±5°.

The process of monitoring detonation initiation in the demining the detonation tube of the device was carried out using three PCB 113B2 pressure sensors, positioned along the tube at intervals of 0.15 m. The distance from the first sensor to the closed end of the detonation tube is 0.4 m. The sensors are powered by a DC source. Signals were stored on a RIGOL DS1104Z Plus oscilloscope. Signals are scanned along the signal front from the 1st channel of the pressure sensor.

Figure 7 shows an experimental setup for measuring the pressure of the shock wave along the detonation tube (a); measuring the pressure of the shock wave on the surface (b); fuze destruction test (c, d).

RESULTS AND DISCUSSION

Numerical results

The qualitative results of the calculations are illustrated in Figure 8, which depicts the destruction of the fuse for three different impulse values at the end of the simulation. The final simulation

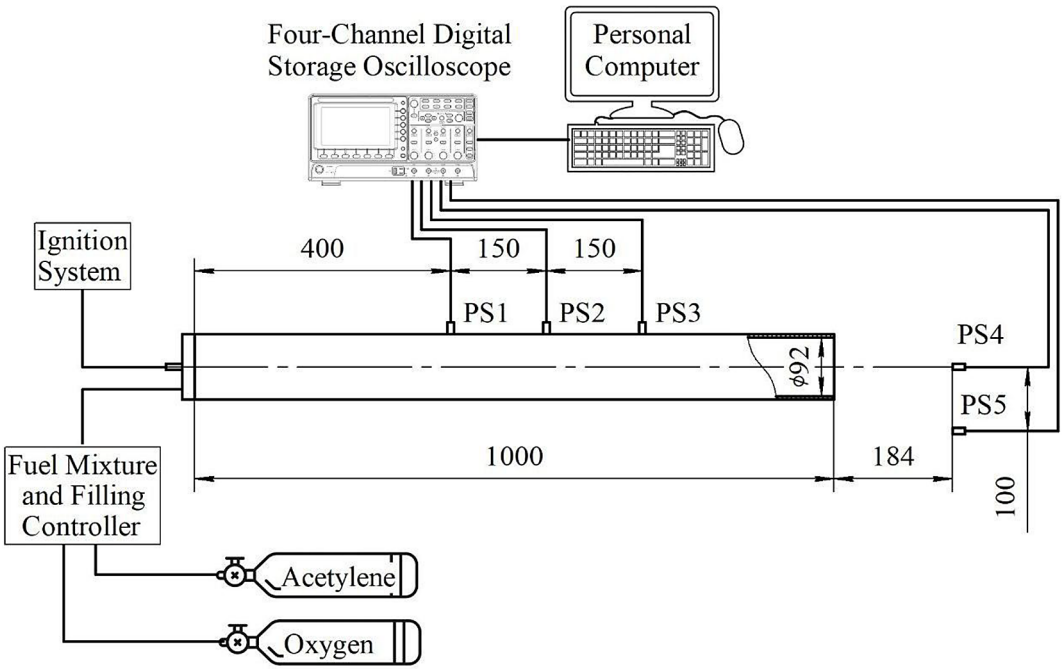

Figure 6. Experimental setup scheme. Distance between pairs of sensors in mm

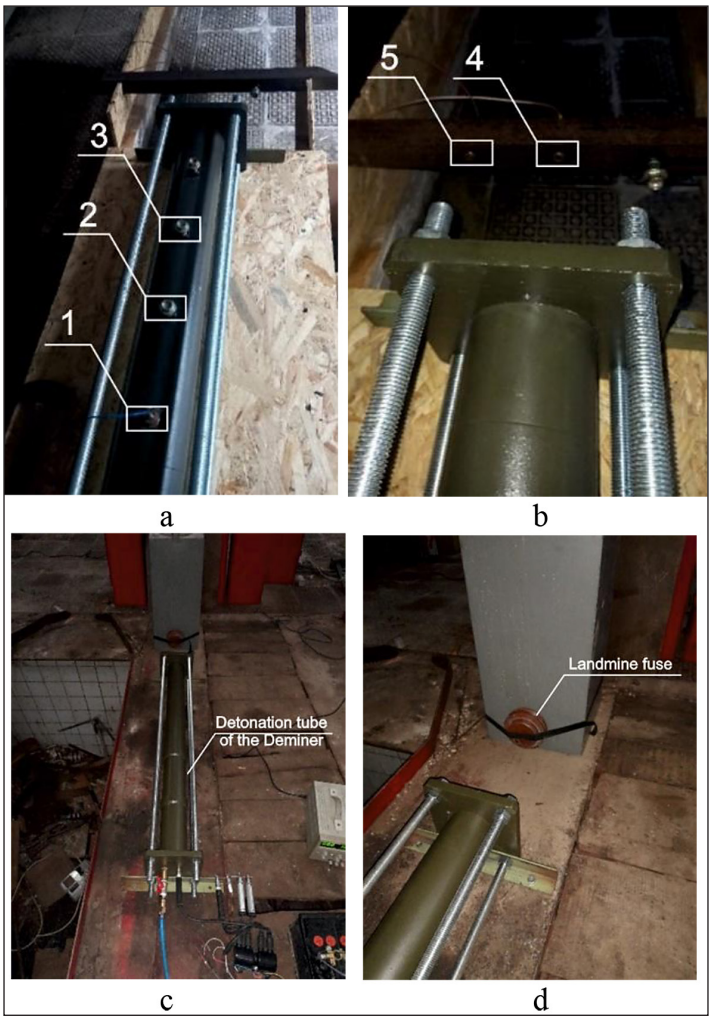

Figure 7. Experimental setup: (a, b) location of pressure sensors according to Figure 6; (c, d) location of the detonation tube of the demining device and the mine fuze

time was determined either by the destruction of the striker (detonator actuation) or, as it was shown in Figure 8c, when the destruction of the striker did not occur, but the values for kinetic and internal energies stabilized.

The quantitative results are presented in Figure 9, which features graphs illustrating the changes in kinetic and internal energy of the fuze components under the shock wave action.

As anticipated, the magnitude of the impulse plays a crucial role in determining the destructive force of the shock wave. This is confirmed both by the fracture patterns (Figure 8) and by the kinetic energy acquired by the fuze components under the action of the shock wave (Figure 9a).

At a high impulse (170.4 Pa·s), not only the plate and the striker but also the housing components are destroyed (Figure 8a). The kinetic energy in this scenario reaches 7 J (as shown in Figure 9a, blue graph), and following the peak value, the internal energy increases due to the additional loading on the housing elements from the pressure plate fragments (see Figure 9b, blue graph). With a low impulse of 36.0 Pa·s, the pressure plate is destroyed, but there is not enough inertia to activate the fuse striker (break off the "eye"). In this case, energy stabilisation occurs immediately after the peak load (see Figure 9b, orange graph). With an increase in impulse to 43.8 Pa·s, the fuze is triggered.

The effect of the shock wave amplitude on the fuse is less pronounced yet remains influential. Increasing the amplitude has a minimal effect on the internal energy level (see Figure 9d), but it increases the kinetic energy of the fuse lid (as shown in Figure 9c), complicating the fuze operation. In this study, the fuze was successfully triggered in all four cases.

Supporting these conclusions, the graphs showing the time interval from the onset of the shock wave to the moment of detonation were presented (see Figure 10). It was observed that reducing the amplitude of the blast wave from 3 MPa to 0.7 MPa increases the delay in detonation from 0.45 ms to 0.8 ms, and detonation eventually occurs. Furthermore, a decrease in the blast wave impulse from 170 Pa·s to 44 Pa·s leads to a sharp increase in the delay in detonation from 0.23 ms to 1.1 ms, while at impulse of 36 Pa·s, detonation does not occur.

Test results

The results of pressure measurements in the detonation tube are shown in Figure 11. The oscillogram indicates that the time intervals between pressure surges at sensors PS 1 and PS 2, as well as between sensors PS 2 and PS 3, are 64 ± 2 μs. Given the distance of 0.15 m between the sensors, the calculated shock wave velocity is 2343 ± 70 m/s. According to reference [20], in a stoichiometric mixture of acetylene and oxygen under normal conditions, the speed of the Chapman-Jouguet detonation wave is 2302 m/s. This suggests that the shock wave detected by the pressure sensors is indeed a detonation wave.

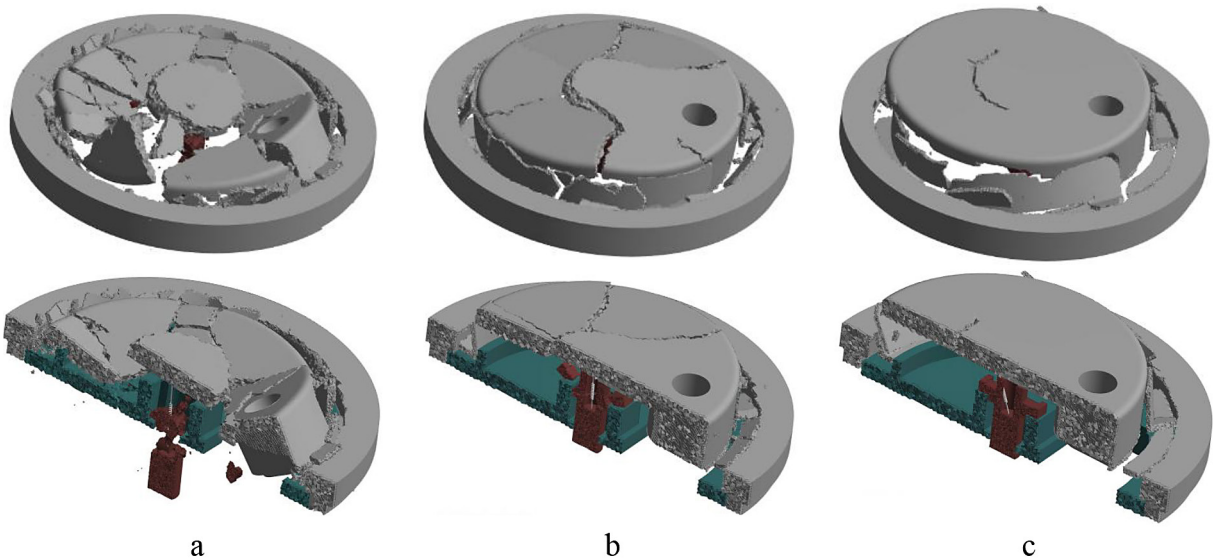

Figure 8. Destruction of the fuse for three levels of explosive wave impulses: (a) high impulse (170.4 Pa·s); (b) moderate impulse (65.6 Pa·s); (c)-low impulse (36.0 Pa·s)

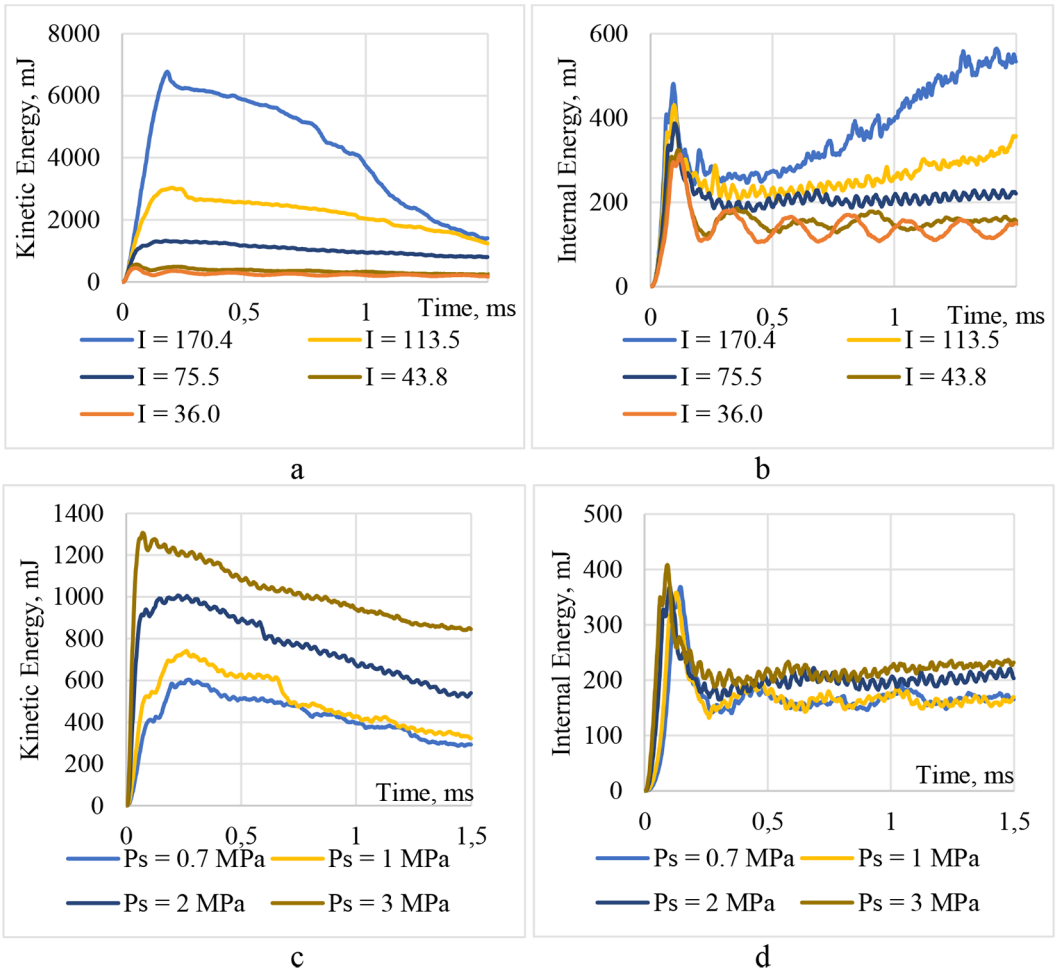

Figure 9. The kinetic and internal energy of the fuze elements: (a, b) when the shape of the shock waves corresponds to Figure 5c; (c, d) when the shape corresponds to Figure 5d

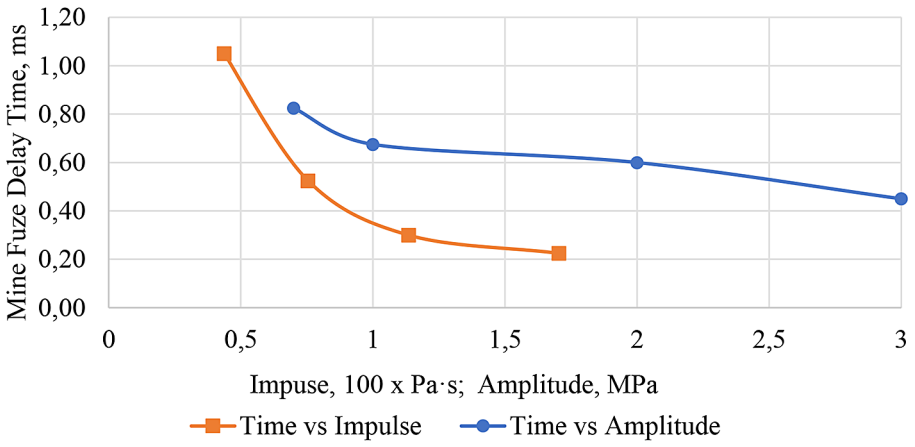

Figure 10. Delay time of mine fuse initiation relative to the onset of the shock wave

Additionally, the amplitude values of the voltage recorded by the sensors are as follows: 480 mV for the first sensor, 360 mV for the second, and 460mV for the third. Given a sensor sensitivity of 0.145 mV/kPa, the corresponding pressure amplitudes are 3.3 MPa, 2.5 MPa, and 3.2 MPa, respectively. These pressure values are consistent with what is expected during a detonation wave under the tested conditions, thereby confirming the occurrence of detonation within the detonation tube.

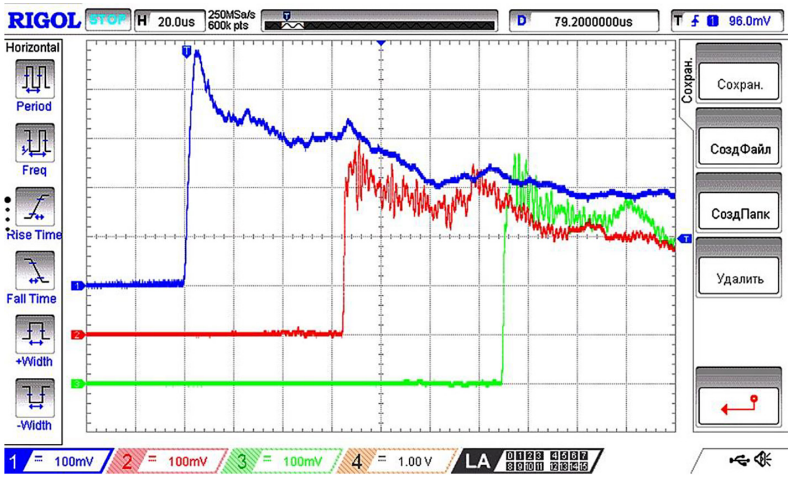

Figure 11. Pressure measurement results in sensors according to Figure 6: PS 1 (blue), PS 2 (red), PS 3 (green)

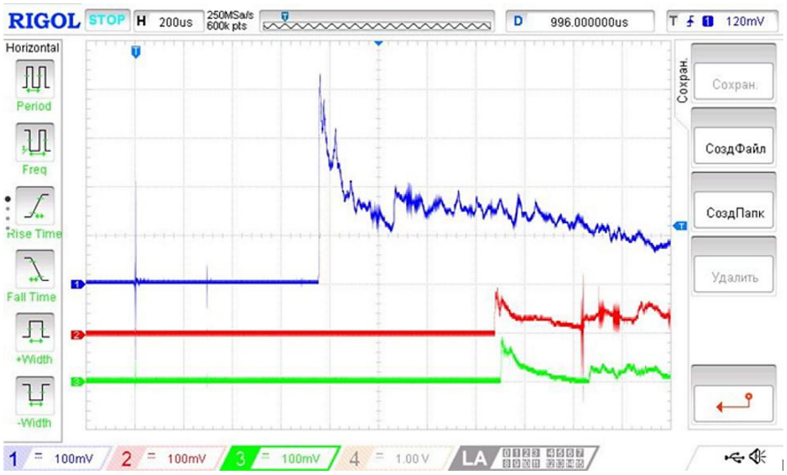

a

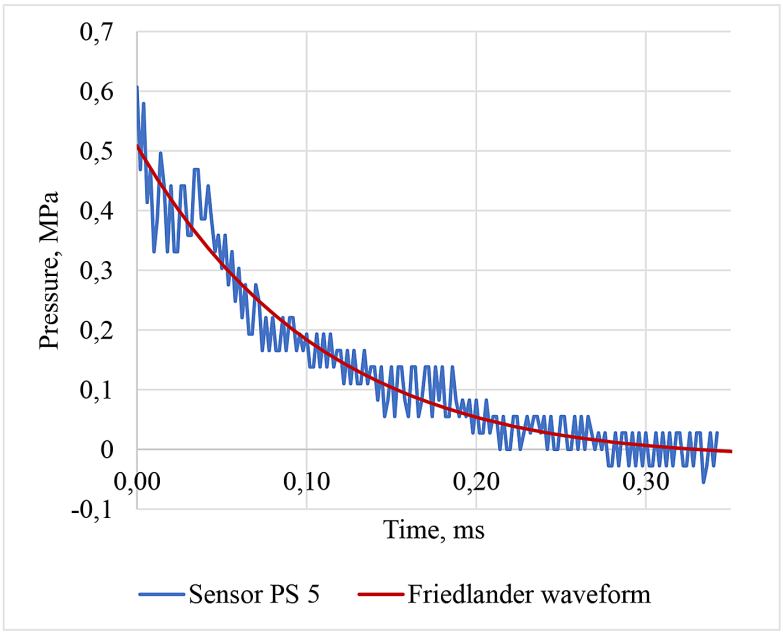

b

Figure 12. Pressure measurement results: (a) PS 1 (blue), PS 4 (red), PS 5 (green); (b) PS 5: experimental and approximate Equation 1

Figure 13. Destruction of the landmine fuze: (a) experiment; (b) numerical modelling

Furthermore, the impact of the detonation products was investigated. Pressure measurements were taken simultaneously inside the detonation tube (as shown in Figure 7a) and outside the tube (Figure 7b). Two pressure sensors were positioned outside the tube; one aligned with the axis of the tube and the other placed 0.1 m to the side (Figure 7b). The distance between the end of the tube and the plane where the pressure was measured was varied during the experiment. Figure 12 shows the pressure graphs in sensors PS 1, PS 4 and PS 5 according to Figure 6, when this distance was 0.368 m and corresponds to four diameters of the detonation tube.

The signal sweep observed is attributed to electromagnetic noise, likely resulting from the operation of the spark ignition system. This indicates that the time taken for the transition from combustion to detonation does not exceed 480 μs. A voltage amplitude of approximately 92 mV was recorded in sensor PS 4, which is located on the axis of the tube (see Figure 6). This corresponds to a pressure of 0.63 MPa. In sensor PS 5, positioned on the side, the maximum pressure reached about 0.61 MPa (88 mV). The small difference in readings between PS 4 and PS 5, along with the proximity of their peak values, suggests a uniform pressure distribution; therefore, the influence of the spherical shape of the blast wave can be disregarded.

Figure 12b displays the readings from sensor PS 5, converted to pressure and real time, along with the approximation of this data using the Friedlander curve (1). The constants used to define the curve were determined using the least squares method and had the following values: P_s = 0.508 MPa, T_s = 0.330 ms, and b = 2.158. It is evident that the Friedlander waveform fits the experimental data well, further confirming the detonation nature of the pressure distribution over time.

The calculated impulse of the shock wave, using formula (2), is 45.8 Pa·s. Direct integration of the experimental curve via the trapezoidal method results in a value of 47.9 Pa·s, which, as discussed in Section 3.1, is sufficient to break the fuze cover.

The results of the fuze destruction experiment are illustrated in Figure 13a, while the numerical modelling results under pressure are shown in Figure 13b. When comparing the fracture patterns, it is evident that, despite their notable similarities, the numerical simulation exhibits more pronounced cracks than the experimental results. This discrepancy can be attributed to the idealised model of the material used in the simulation. Unlike in the model, the actual material is inhomogeneous and has some plasticity, whereas the simulation assumes isotropy and perfect brittleness of the material.

CONCLUSIONS

To investigate the influence of shock wave parameters on the operation and destruction mechanisms of landmine fuses, a comprehensive computational and experimental study was conducted.

A finite element model of the fuze was developed, with detailed justification for the selected geometric configuration, discretization parameters, and material properties. The mesh size was optimised to ensure numerical stability and accuracy, while the boundary conditions were defined to replicate realistic loading and support conditions of the fuse during detonation.

The temporal profile of the applied pressure was described using the Friedlander waveform,

which accurately represents the overpressure characteristics associated with blast phenomena. Parametric analysis demonstrated that the duration of the positive phase and the decay coefficient are interdependent parameters that exert only a minor influence on the waveform shape. Consequently, two primary simulation scenarios were considered: (i) variation of the impulse at a constant pressure amplitude, and (ii) variation of the amplitude at a constant impulse.

The results indicated that the destructive capacity of the shock wave is predominantly determined by its impulse, which must reach at least 40 Pa·s to reliably initiate or destroy the fuse. Although the amplitude of the pressure pulse has a comparatively smaller effect, higher amplitudes were observed to increase the degree of mechanical damage to the fuse components. Experimental measurements obtained from pressure sensors in the demining device confirmed stable detonation of a stoichiometric oxygen-acetylene mixture within the demining tube. The recorded pressure distribution across the surface of the mine fuze was found to be nearly uniform and well described by the Friedlander function, validating the applicability of the adopted blast wave model. Furthermore, the experimentally obtained threshold values of the blast wave impulse required for fuze destruction were consistent with theoretical predictions, confirming the reliability of the developed numerical model.

Future research will focus on increasing the blast wave impulse and, consequently, enhancing the effective standoff distance between the demining device and the mine. This approach aimed to reduce the mechanical and thermal impact of the shock wave on the demining device structure while maintaining sufficient energy transfer for effective landmine fuze initiation.

Acknowledgments

This study has funded by the National Research Foundation of Ukraine under granting the Project No. 2023.04/0027. Authors express gratitude to CADFEM UA LLC, the Channel Partner of Ansys Inc. in Ukraine, for help with the software licensing.

REFERENCES

1. Mikulic D. Design of Demining Machines. In: Design of Demining Machines. London: Springer; 2012; 73–152. https://doi.org/10.1007/978-1-4471-4504-2_3
2. Zaichenko, S., Vovk, O., Voitenko, Y., Li, M.: Analysis and Prospects for the Development of Humanitarian Demining Methods. In: Babak, V., Zaporozhets, A. (eds) Systems, Decision and Control in Energy VII. Cham: Springer, 2025. https://doi.org/10.1007/978-3-031-90466-0_38
3. Pratt, D., Torbet, N.: The hybrid thermal lance: A promising new technique for the destruction of landmines and UXO by deflagration. Journal of Conventional Weapons Destruction 2018; 22(2), 7.
4. Vega, F., Roman, F., Pantoja, J., Peña, N., Mora, N., Rachidi, F.: High power electromagnetics applied to humanitarian demining in Colombia. In: USNC-URSI Radio Science Meeting, 2016; 33–34. https://doi.org/10.1109/USNC-URSI.2016.7588498
5. Wang, B., Rao, Z., Xie, Q., Wolański, P., Rarata, G.: Brief review on passive and active methods for explosion and detonation suppression in tubes and galleries. J. Loss Prevention Process Ind. 2017; 49, 280–290. https://doi.org/10.1016/j.jlp.2017.07.008
6. Tabassum, Z., Banu, S., Fathima, N., Fathima, A., Aiman, M.: Revolutionizing Post-Conflict Landmine Clearance with UAV Technology. ICNEWS, 2024; 1–8. https://doi.org/10.1109/ICNEWS60873.2024.10730928
7. Myntiuk V., Tkachenko D., Pavlenko O., Shypul O. Simulating the Effect of Mine Explosion on a Remote Gas Detonation Deminer. In: Lecture Notes in Networks and Systems. Cham: Springer; 2025; 443–54. https://doi.org/10.1007/978-3-031-94852-7_37
8. Pavlenko O., Shypul O., Myntiuk V., Tkachenko D., Brega D., Garin V. Development of a conceptual model for a gas detonation deminer. Aerospace Technic and Technology. 2024; 6: 70–9. https://doi.org/10.32620/aktt.2024.6.07
9. Kalinko D., Łopatka M., Rubiec A., Krogul P. Simulations of the ground pressure exerted by demining rollers with rigid wheels. Adv Sci Technol Res J. 2024; 19(2): 163–78. https://doi.org/10.12913/22998624/195451
10. Offermanns H, Retzlaff F. Bakelit: der erste seiner Klasse. Nachrichten Aus Der Chemie. 2020; 68(6): 10–3. https://doi.org/10.1002/nadc.20204099964
11. Liu Y., Yang Z., Jiang C., Xu D., Qiu H., Gao L. Lightweight design optimization of two-layer corrugated cored sandwich panel under blast loading using surrogate-assisted different evolution for mixed-integer variables. Eng Struct. 2024; 321: 118963. https://doi.org/10.1016/j.engstruct.2024.118963
12. Patel M., Patel S. Determination of high-strength polymer composite reinforcement effect on the armor-grade aluminum plates' explosion resistance—A computational perspective. Polym Compos. 2024; 46(4): 3770–90. https://doi.org/10.1002/pc.29205
13. Gargano A., Mouritz A. Comparative study of the

explosive blast resistance of metal and composite materials used in defence platforms. Compos Part C Open Access. 2023; 10: 100345. https://doi.org/10.1016/j.jcomc.2023.100345

14. Gabriel S., Langdon G.S., von Klemperer C.J., Kim Yuen S.C. Blast behaviour of fibre reinforced polymers containing sustainable constituents. J Reinf Plast Compos. 2022; 41(19–20): 771–90. https://doi.org/10.1177/07316844211072529
15. Ravindran S., Gandhi V., Lawlor B., Ravichandran G. Mesoscale shock structure in particulate composites. J Mech Phys Solids. 2023; 174: 105239. https://doi.org/10.1016/j.jmps.2023.105239
16. Shah S., Hazell P.J., Wang H., Escobedo J.P. Shock wave mitigation in heterogeneous systems: A review. J Dyn Behav Mater. 2025. https://doi.org/10.1007/s40870-025-00466-w
17. LS-DYNA® Homepage. Available from: https://lsdyna.ansys.com [cited 2025 Jul 20].
18. LS-DYNA®. Keyword User's Manual. Vol. I. Livermore Software Technology (LST), an ANSYS Company; 2025.
19. LS-DYNA®. Keyword User's Manual. Vol. II Material Models. Livermore Software Technology (LST), an ANSYS Company; 2025.
20. Lewis B., von Elbe G. Combustion, flames and explosions of gases. 2nd ed. New York: Academic Press; 1961. https://doi.org/10.1016/C2013-0-12402-6